Nano-porous anodic aluminium oxide membranes with 6–19 nm pore diameters formed by a low-potential anodizing process

This content has been downloaded from IOPscience. Please scroll down to see the full text.

2007 Nanotechnology 18 345302

(http://iopscience.iop.org/0957-4484/18/34/345302)

View the table of contents for this issue, or go to the journal homepage for more

Download details:

IP Address: 111.207.250.57
This content was downloaded on 31/05/2017 at 13:41

Please note that terms and conditions apply.

You may also be interested in:

Formation of nanoporous titanium oxide films on silicon substrates using an anodizationprocess
Xiaofeng Yu, Yongxiang Li, Wanyin Ge et al.

Highly ordered porous alumina with tailor-made pore structures fabricated by pulseanodization
Woo Lee and Jae-Cheon Kim

Fabrication of novel porous anodic alumina membranes by two-step hard anodization
Y Li, Z Y Ling, S S Chen et al.

Permeability of anodic alumina membranes with branched channels
D I Petukhov, K S Napolskii and A A Eliseev

Size control of highly ordered HfO2 nanotube arrays and a possible growth mechanism
Xiaofeng Qiu, Jane Y Howe, Mateus B Cardoso et al.

Cyclic voltammetry as a tool to estimate the effective pore density of an anodic aluminiumoxide template
Xiaoli Cui, Qiang Zhao, Zhizhou Li et al.

Fabrication of anodic aluminium oxide templates on curved surfaces
Aijun Yin, Rodney S Guico and Jimmy Xu

Self-ordering behavior of nanoporous anodic aluminum oxide (AAO) in malonic acidanodization
W Lee, K Nielsch and U Gösele

Fast fabrication of self-ordered anodic porous alumina on oriented aluminum grains by high acid concentration and high temperature anodization
Chuan Cheng and Alfonso H W Ngan

IOP PUBLISHING NANOTECHNOLOGY
Nanotechnology **18** (2007) 345302 (4pp) doi:10.1088/0957-4484/18/34/345302

Nano-porous anodic aluminium oxide membranes with 6–19 nm pore diameters formed by a low-potential anodizing process

Fan Zhang, Xiaohua Liu, Caofeng Pan and Jing Zhu[1]

Beijing National Center for Electron Microscopy, Tsinghua University, Beijing 100084,
People's Republic of China
and
Laboratory of Advanced Materials, Department of Materials Science and Engineering,
Tsinghua University, Beijing 100084, People's Republic of China

E-mail: jzhu@mail.tsinghua.edu.cn

Received 27 April 2007, in final form 5 June 2007
Published 27 July 2007
Online at stacks.iop.org/Nano/18/345302

Abstract

Self-organized nano-porous anodic aluminium oxide (AAO) membranes with small pore diameters were obtained by applying a low anodizing potential in sulfuric acid solutions. The pore diameters of the as-prepared AAO membranes were in the range of about 6–19 nm and the interpore distances were about 20–58 nm. Low potentials (6–18 V) were applied in anodizing processes to make such small pores. A linear relationship between the anodizing potential (U_a) and the interpore distance (D_{int}) was also revealed. By carefully monitoring the current density's evolution as a function of time with different U_a (2–18 V) during the anodizing processes, a new formula is proposed to simulate the self-ordering anodizing process.

(Some figures in this article are in colour only in the electronic version)

1. Introduction

Nano-porous anodic aluminium oxide (AAO) membranes have been widely used as templates in the synthesis of one-dimensional (1D) nanomaterials or quantum dot (QD) arrays [1]. This low-cost membrane has attracted much interest for its wide use and high efficiency. Various nanostructures have been created within the membranes, such as solar cells [2], carbon nanotubes [3], catalysts [4], metal nanowires [5, 6] and heterojunctions [7]. However, all of the AAO membranes previously reported were merely prepared under high anodizing potentials (19–160 V). As a result, the interpore distances were generally in the range of 50–500 nm [8, 9]. Here, we report AAO membranes with pore diameters varying from 6 to 19 nm synthesized by applying comparatively lower anodizing potentials of 6–18 V. In this case, the interpore distances are proportional to the applied anodizing potential and vary in the range of 20–58 nm, which can be used to fabricate 1D nanomaterial arrays of high density. Furthermore, a new formula is established based on the current-density-monitoring experiments with varying anodizing potentials ranging from 2 to 18 V. It helps us to understand the self-ordered anodizing process. With increasing time, the current density is observed to initially decrease and start to increase within 20 s. As the anodizing process proceeds, the current density stops growing and begins to re-drop at a certain time (so-called 'peak-time'), indicating that the pores' growth rate arrives at the highest level around the peak-time. The peak-time becomes shorter with increasing anodizing potential indicating that pores grow faster at higher potentials.

2. Experimental details

The aluminium (Al) foil of high purity (99.99%) was firstly cut into small pieces (3 × 4 cm^2) and annealed in a furnace in

---

[1] Author to whom any correspondence should be addressed.

air at 600 °C for 2 h. The Al plates were chemically polished in a mixed acid solution (H_3PO_4:HNO_3:H_2O = 8:1:1, volume) at 95 °C for 30 s, followed by electrochemical polishing in a perchloric acid ethanol solution ($HClO_4$:C_2H_5OH = 1:4, volume). A two-step anodizing process was adopted afterwards [10]. Anodizing was conducted under a constant potential in H_2SO_4 aqueous solution (10 wt%). The potential was respectively set at 6, 8, 9, 12, 16, and 18 V for the pore diameter measuring experiments and set at 2, 4, 6, 9, 12, 14, 16, and 18 V for the current density monitoring experiments. The Al plate was fixed in the acid solution, at a distance of 10 cm from the cathode of a mechanically polished copper (Cu) plate. The temperature was kept at 3 °C by using an icy water bath during the experiments. The oxide layer produced by the first anodization of 12 h was chemically removed by submerging the Al plate in a chromic acid solution (H_3PO_4:CrO_3:H_2O = 3:1:41, weight). The second anodization was applied under identical conditions to the first anodization but with a shorter duration of 3 h [11].

3. Results and discussion

With a fixed 10 wt% H_2SO_4 aqueous solution, nanochannels with different pore diameters can be obtained by applying different anodizing potentials. In this series of experiments, different pore diameters ranging from 6.8 to 19.34 nm were obtained under various potentials ranging from 6 to 18 V. Figures 1(a)–(e) show FE-SEM micrographs of the as-prepared AAO membranes with average pore diameters of 6.8, 8.6, 11.12, 16.38 and 19.34 nm by applying anodizing voltages of 6, 8, 12, 16 and 18 V, respectively. The inset of figure 1(a) shows that the AAO membrane's hexagonal feature can always be seen even when an ultra-low anodizing potential (6 V) is used. Note that the AAO membrane's growth is more sensitive to outside disturbance at low anodizing potentials. Although the pore arrays remain ordered, the pore diameter and shape fluctuate more easily when the anodizing potential decreases.

Previous studies suggested that the anodizing potential has a major effect on both pore diameter and interpore distance when a high potential is applied. The relation can be expressed as $D_{\text{int}} = 2.81U_{\text{a}} - 1.7$ [12], with D_{int} being the interpore distance and U_{a} being the anodizing potential. However, the relationship between pore diameters and the potential for lower potentials remains unexplored. Based on our investigations of the AAO membranes anodized under low potentials, we find that in this regime, the pore diameter exhibits a similar linear relationship with the anodizing potential but a different proportionality factor of 0.9666 (figure 2). The relation between interpore distance and the applied potential is determined to be $D_{\text{int}} = 2.97U_{\text{a}} + 2.49$ following the 10% porosity rules [13]. The porosity of the AAO structure is given by $P = \frac{2\pi}{\sqrt{3}}(\frac{r}{D_{\text{int}}})^2$ with P being the porosity and r being the pore radium, in which P is a constant of 10%. Thus we can work out $r = 0.166D_{\text{int}}$ for our experiments. It can be seen that the proportionality is almost the same for the low-U_{a} synthesized AAO membranes as for the high-U_{a} ones. The positive intercept shows that the acid resolution ability significantly affects the small pores' formation, in contrast to the negative intercept for large pores formed under high potentials.

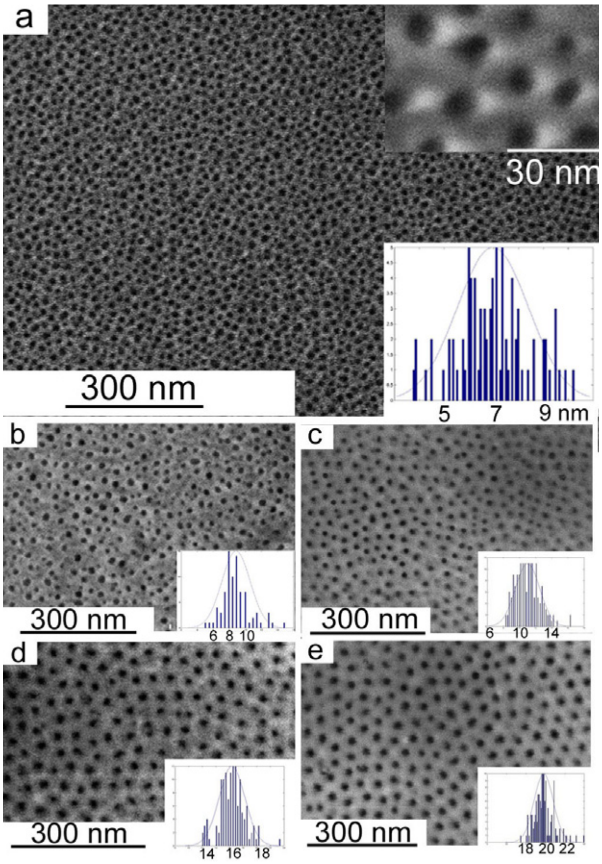

Figure 1. Plan view SEM micrographs of the AAO membranes. The periodic pore arrangements with pore diameters of (a) 6.8, (b) 8.6, (c) 11.12, (d) 16.38 and (e) 19.34 nm are obtained under anodizing potentials of 6, 8, 12, 16 and 18 V, respectively. The inset histograms show the Gaussian distributions of the pore diameters for the five samples. Two magnified figures are inset in (a) for clarity. The images in (a) and (b) were taken using a HITACHI S-5500 FE-SEM instrument and the others using a JOEL JSM-6301F.

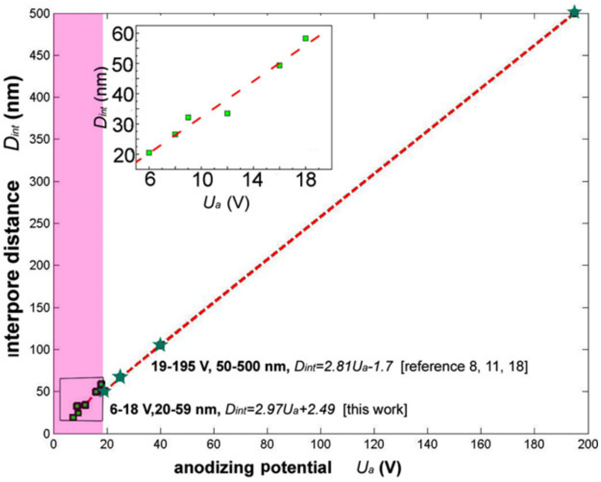

Figure 2. Relationship of the interpore distance (D_{int}) and the anodizing potential (U_{a}). Data from the present work are plotted in the pink zone, fitting to a formula of $D_{\text{int}} = 2.97U_{\text{a}} + 2.49$, while data from [8, 11, 18] are plotted in the blank zone with another fitting formula of $D_{\text{int}} = 2.81U_{\text{a}} - 1.7$ for comparison. The inset shows a magnified view of the rectangle-enclosed part. The interpore diameters are 20.47, 25.89, 32.13, 33.49, 49.33, and 58.25 nm under lower anodizing voltages of 6, 8, 9, 12, 16 and 18 V, respectively.

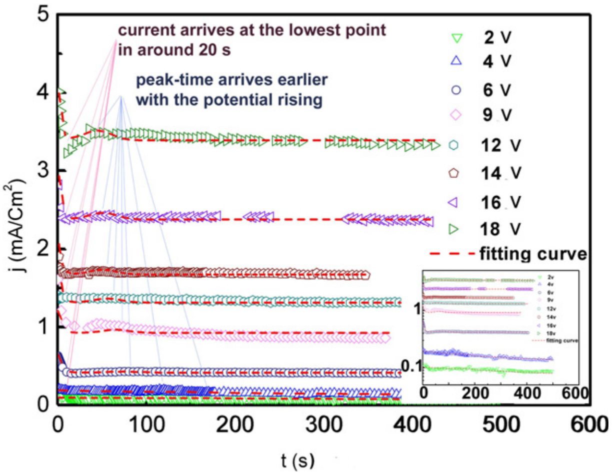

Figure 3. Experimental results of the relationship between current density and time. The inset shows the same results but with a logarithmic vertical axis. It can be seen that the current drops fast at the beginning and arrives at a low point in about 20 s. Then it rises a little for a period depending on the anodizing voltage to the peak before re-dropping. A new pore-growth model is set up to describe such a process which corresponds well with the experimental results.

The interpore distances, D_{int}, are assumed to be related to the anodizing potential as follows:

$$D_{\text{int}} = \xi U_{\text{a}} = (C_{\text{pore}} + C_{\text{wall}})U_{\text{a}} \tag{1}$$

where C_{wall} is the coefficient determining the wall thickness and depends on the barrier thickness, τ_{barrier}, through the relation $C_{\text{wall}} = \zeta_{\text{wall}}\tau_{\text{barrier}}$. C_{pore} is the coefficient on which the pore diameter depends. Generally, the products of $C_{\text{pore}}U_{\text{a}}$ and $C_{\text{wall}}U_{\text{a}}$ are the pore diameter and the wall thickness, respectively [14]. Furthermore, according to Cabrera and Mott's theory on the electric properties of Al film [15], the barrier thickness, the anodizing potential and the current density (j) are related to one another by the following equation:

$$j = j_0 \exp(\beta U_{\text{a}}/\tau_{\text{barrier}}) \tag{2}$$

where j_0 and β are both material and temperature dependent parameters. It can be referred that the parameters j and U_{a} play important roles in the anodizing process.

In order to gain a better understanding of the formation mechanism of the AAO membranes, we further studied the current density evolution with increasing time for different anodizing potentials of 2–18 V. Our experimental results show that the current density varies with the anodizing potential as well as the anodizing time. The anodizing potential is a dominant factor when the current density becomes stable, while the anodizing time is a crucial parameter affecting the current density largely at the very beginning. By monitoring the current density evolution as a function of time, we could understand the self-anodizing process in the anodizing potential range. Figure 3 shows the experimental j–t curve illustrating the current density evolution. Initially the current density decays fast and reaches a minimum in a short duration (within ~20 s). Then it increases to a maximum at the so-called peak-time. The higher the potential applied, the more quickly the peak-time point appears. After the peak-time, the current density decreases slightly and eventually becomes stable at a certain value, which depends on the anodizing potential.

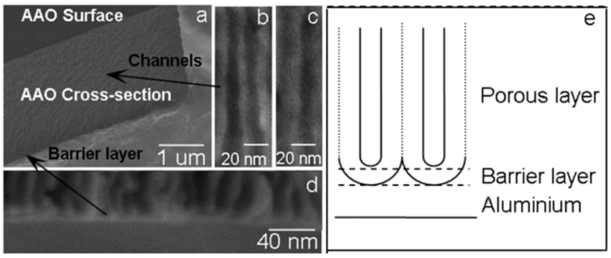

Figure 4. FE-SEM micrographs and a schematic diagram showing the cross-section of an AAO membrane. (a) FE-SEM image (HITACHI S-5500) showing a general cross-section view of the membrane synthesized at 6 V; (b) and (c) magnified images of the channels; (d) magnified image of the barrier layer; (e) schematic diagram of AAO membrane's cross-section.

These j–t curves in figure 3 give much useful information on the growth process of the AAO membranes. It is well known that an AAO membrane is a combination of two layers, i.e. a barrier layer and a porous layer [16]. However, so far no model has been set up to describe the whole AAO growth process. Based on our experimental results we can obtain some details about the AAO growth. In the first 20 s, the current density drops quickly. This indicates that a barrier layer of high resistance is formed during this period. After that, pores begin to appear on the surface of the barrier and penetrate the old barrier layer with a new barrier layer frontier in the growth direction. Pores grow fastest at a certain time (the peak-time) and the current density shows a peak, whose position is dependent on the applied anodizing potential. It is for this reason that small peaks are always seen in the j–t curves for all experiments with varying anodizing potentials. Finally, the breakdown of the old barrier layer and the growth of the new barrier layer reach a balance as the porous layer grows thicker with increasing time. Figure 4 shows a cross-section of the final AAO membrane fabricated at 6 V. The pores, of cylindrical cross-section, are separated from the macroscopic aluminium surface by a relatively compact barrier layer of scalloped appearance.

Hereafter, a new formula is established to describe such a process which agrees well with the experimental results:

$$j = A\exp(-t/B) + \frac{C}{t}\exp[-(t-\tau)^2/2\omega^2] + j_0 \tag{3}$$

where j, t and j_0 are the current density, time, and the residue current density, while A, B and C are the coefficients, respectively. The first part of equation (3), $A\exp(-t/B)$, describes the influence of the barrier layer on the current density. The current density decays exponentially with the time in such a process according to Zakgeim's theory [17]. The second part of equation (3), $\frac{C}{t}\exp[-(t-\tau)^2/2\omega^2]$, describes the porous layer's influence on the current density. The exponential part, $\exp[-(t-\tau)^2/2\omega^2]$, is a Gaussian distribution which means the pores start to grow in a certain time τ after the beginning of this anodizing process. In fact, the pores cannot grow until the initially formed barrier is penetrated and the current density increases as a result. More pores form in the AAO, the higher the current density is. On

Table 1. The fitting parameters for the j–t curves in figure 3.

U_a (V)	A (A cm^{-2})	B (s)	C (A (cm^2 s)$^{-1}$)	τ (s)	ω (s)	j_0 (A cm^{-2})
2	0.05	800	0.6	150	20	0.053
4	0.07	300	0.9	100	20	0.128
6	0.2	5	1.05	80	20	0.42
9	0.35	4.5	2.8	70	20	0.914
12	0.4	3.8	3	60	15	1.34
14	0.55	3.65	3.2	55	15	1.68
16	0.75	3.2	4.5	55	15	2.38
18	0.8	3	6	50	15	3.39

the other hand, the porous layer's thickness grows linearly with time. As the layer becomes thicker, it becomes more difficult for ions to pass through which causes the current density's decay. This phenomenon is expressed by C/t with C being the coefficient proportional to the applied potential.

By fitting the experimental results with equation (3), the parameters are retrieved and listed in table 1.

The experimental results show that with rising U_a the parameters A, C and j_0 increase whereas B and τ decrease. The factor B increases when the anodizing potential drops. When an extremely low anodizing potential (<5 V) is applied, the barrier layer grows very slowly. The value of τ changes from 150 to 50 s with the rising potential. It can be referred to as a faster launch of the porous layer when a higher potential is used. On the other hand, ω does not vary a lot, consistent with the fact that the pores' launch process usually lasts for just ~20 s and after that the porous layer becomes thicker but the number of pores remains fixed.

4. Conclusions

A linear relationship between the anodizing potential (U_a) and the interpore-distance (D_{int}) is found for the AAO membranes synthesized under low-U_a (6–18 V) by a two-step method. The proportionality of the D_{int}–U_a relation is about 3. The current density evolution is monitored during the anodization processes with potentials of 2–18 V, based on which a formula is established to describe the self-ordered anodizing process of AAO. Our results show that the AAOs formation initiates with a porous layer launch process that usually lasts for ~20 s. The launch of the porous layer becomes quicker when a higher anodizing potential is used. When an extremely low anodizing potential (<5 V) is applied, the barrier layer grows much more slowly than that with high potentials applied.

Acknowledgments

This work was supported by the National 973 Project of China, the Chinese National Nature Science Foundation, and the National Center for Nanoscience and Technology of China.

References

[1] Shingubara S 2003 *J. Nanopart. Res.* **5** 17
[2] Karmhag R, Tesfamichael T, Wackelgard E and Niklasson G A 2000 *Sol. Energy* **68** 329
[3] Che G, Lakshmi B B, Fisher E R and Martin C R 1998 *Nature* **393** 346
[4] Che G, Lakshmi B B, Martin C R, Fisher E R and Ruoff R S 1998 *Chem. Mater.* **10** 260
[5] Liu X H, Luo J and Zhu J 2006 *Nano Lett.* **6** 408
[6] Zhang Z B, Gekhtman D, Dresselhaus M S and Ying J Y 1999 *Chem. Mater.* **11** 1659
[7] Luo J and Zhu J 2006 *Nanotechnology* **17** S262
[8] Masuda H, Hasegwa G and Ono S 1997 *J. Electrochem. Soc.* **144** L127
[9] Li A P, Müller F, Birner A, Nielschm K and Gösele U 1998 *J. Appl. Phys.* **84** 6023
[10] Masuda H and Satoh M 1996 *Japan. J. Appl. Phys.* **35** L126
[11] Zhang X 2003 *Thesis* Tsinghua University
[12] Ebihara K, Takahashi H and Nagayama M 1983 *J. Met. Finishing Soc. Japan* **34** 548
[13] Nielsch K, Choi J, Schwirn K, Wehrspohn R B and Gosele U 2002 *Nano Lett.* **2** 677
[14] Lee W, Ji R, Gosele U and Nielsch K 2006 *Nat. Mater.* **l5** 741
[15] Cabrera N and Mott N E 1949 *Rep. Prog. Phys.* **12** 163
[16] Keller F, Hunter M S and Robinson D L 1953 *J. Electrochem. Soc.* **100** 411
[17] Biestek T and Weber J 1976 *Electrolytic and Chemical Conversion Coating* (Redhill, Surrey: Portcullis Press)
[18] Masuda H, Yada K and Osaka A 1998 *Japan. J. Appl. Phys.* **37** L1340